

Evolution of Recrystallization Texture in Aluminum Alloy Sheets by Asymmetric-Warm-Rolling

Yoshikazu Suzuki¹, Osamu Noguchi¹, Yoshiki Miki¹, Yoichi Ueno¹,

Katsumi Koyama¹ and Toshio Komatsubara²

¹ Technical Research Div., Furukawa-Sky Aluminum Corp., 1351 Uwanodai, Fukaya, Saitama 366-8511, Japan

² Casting & Forging Div., Furukawa-Sky Aluminum Corp., 560 Doto, Oyama, Tochigi 323-0812, Japan

Asymmetric-warm-rolling (AWR) is a promising process to improve the Lankford value (r-value) or the deep drawability of aluminum alloy sheets by controlling the crystallographic texture of the alloy. A fundamental study has been conducted on the formation of a distinctive recrystallization texture in the Al–1 mass% Si–0.6 mass% Mg (AA6022) alloy sheets prepared by AWR at 523K. The change in texture during the recrystallization process was observed by using a SEM-EBSD system with a heating stage. The as-AWRed sheets have a considerably recovered subgrain-structure with a major orientation of $\{001\}<110>$ and texture fibers of $<011>/\text{RD}$ and near $<111>/\text{ND}$. Some of the recovered grains act as the nuclei for the recrystallization process and grow consuming adjacent grains. The area fraction of the $<001>/\text{ND}$ grains decreases with grain growth during the multistep-annealing at 573–723K. The $\{112\}$, $\{332\}$ and $\{221\}$ grains increase or remain high in area fraction during the annealing, whereas the fraction of the ideal $\{111\}$ grains decreases. For the T4 sheets made by AWR, not only the ideal $\{111\}$, but the slightly rotated components probably contribute to a high average r-value. Limited area fraction of $\{001\}$ grains is another reason for the high r-value.

Keywords: *Asymmetric-warm-rolling, 6022 alloy, texture, SEM-EBSD, ODF.*

1. Introduction

Light-weight aluminum alloy sheets are inherently useful as auto-body sheets for reducing the weight of automobiles. However, the press formability of aluminum alloy sheets is not as high as that of steel auto-body sheets. Therefore, an improvement in the press formability of aluminum alloy sheets is required for a more widespread use of these sheets.

It is well known that crystallographic texture has significant effects on the press formability of metal sheets. In case of the steel auto-body sheets, the major recrystallization texture components of $<111>/\text{ND}$ or γ -fiber in BCC metals lead to the good deep-drawability and high Lankford value (r-value). In contrast, a major orientation of $\{001\}<100>$ or Cube in the FCC aluminum alloy sheets tends to lower the average r-value.

Some previous papers [1–3] have proposed a technique employing asymmetric-warm-rolling (AWR) in order to improve the formability or r-value of aluminum alloy sheets. AWR has been considered to be a measure to attain a recrystallization texture of $<111>/\text{ND}$ for aluminum alloy sheets. The $\{111\}$ texture is believed to improve formability of aluminum alloy sheets. In fact, an improved r-value of 1.2 has been reported for Al–Mg–Cu alloy sheets by AWR[2], while in general, the average r-values of the sheets by conventional rolling (CR) are 0.6–0.8.

It can be said that the effects of AWR on the improvement of r-value is evident. However, little is known about the evolution of the recrystallization texture of the AWRed aluminum alloy sheets. This study focuses on the formation of the distinctive recrystallization texture of the AWRed sheets, for an Al–Mg–Si alloy AA6022. The changes in texture have been determined for an identical observation area during a multi-step annealing process.

2. Experimental

The alloy used in this study is AA6022, which contains approximately 1 mass% Si and 0.6 mass% Mg (Table 1). The slabs of the alloy were prepared by using a laboratory-scale direct chill (DC) caster. Then, they were homogenized and scalped to a thickness of 100 mm. In the AWR process, we employed a specially designed rolling mill that had independent driving motors and inside heaters for both rolls. The slabs were rolled at 523 K into 1 mm-thick sheets; the asymmetric roll speed ratio was 150%–250%. Silicone-type lubricating oil was applied to the roll surfaces during the rolling in order to prevent adhesion. For comparison, the 6022 alloy sheets were also prepared by CR: the scalped slabs were hot rolled to 6mm and cold rolled to 1mm in thickness.

Table 1 Chemical composition of AA6022 alloy (mass%)

Si	Fe	Cu	Mn	Mg	Ti	Al
1.00	0.10	0.01	0.05	0.55	0.01	Bal.

Comparative texture measurements by an electron backscatter diffraction system (EBSD) attached to a scanning electron microscope (SEM) were carried out for the T4 sheets made by AWR and CR. In the T4 treatment, the sheets were solution-treated at 823K for 300s, water-spray quenched and natural-aged. The EBSD data were summarized in inverse pole figure (IPF) maps and Bunge-type orientation distribution functions (ODF).

The changes in texture of the sheets prepared by AWR and CR throughout the recrystallization process during multi-step annealing were determined by using the SEM-EBSD apparatus with a heating stage. The as-rolled samples were polished mechanically and electrochemically on the L-LT surface. Then, they were heated to 548–723K and cooled in the chamber of the SEM in a multi-step manner (Fig.1). The heating rate in each annealing step was approximately 0.2 K/s. The texture was determined by EBSD for an almost identical observation area at room temperature after each cycle of heating and cooling in the multi-step annealing process.

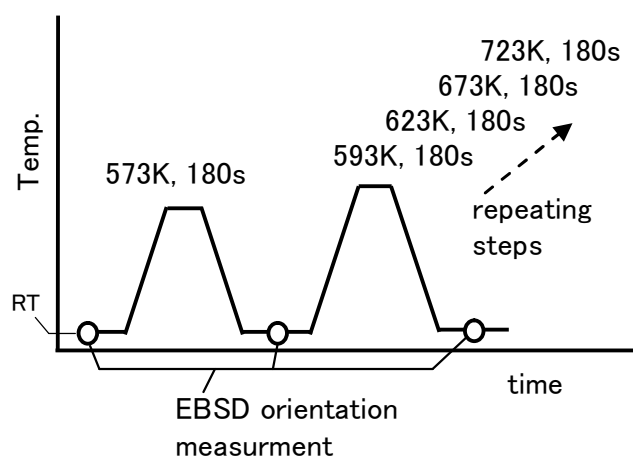


Fig.1 Procedure for multi-step annealing and EBSD orientation measurement.

3. Results and Discussion

3.1 Recrystallization texture of solution-treated T4 sheets

First, the characteristics on the recrystallization texture of the AA6022 alloy T4 sheets by AWR were confirmed as the basis for further discussion. Fig.2 shows IPF-type EBSD maps for the recrystallization structures on the L-ST cross-sections of the T4 sheets prepared by AWR and CR. ODFs calculated from the EBSD data are illustrated in Fig.3.

The T4 sheet made by CR consists mainly of $\langle 001 \rangle$ //ND grains; these grains are represented as red ones in the IPF map. The ODF shows that Cube orientation of $\{001\}\langle 100 \rangle$ is the major recrystallization texture component in the CR sheet. The AA6022 alloy sheet by CR has a low average r -value of 0.6 because of the pronounced $\{001\}$ orientations, including the Cube orientation.

On the other hand, the AWRed sheet includes near $\langle 111 \rangle$ //ND grains throughout the entire sheet thickness; these grains are represented as bluish grains in the IPF map. More precisely, the center of the orientation intensity is not exactly on $\langle 111 \rangle$ //ND but on $\langle 332 \rangle$ or $\langle 221 \rangle$ //ND. The

misorientations of $\{332\}\langle 113\rangle$ and $\{221\}\langle 114\rangle$ from the ideal $\{111\}\langle 112\rangle$ are approximately 10° and 15° , respectively. The orientation intensity of $\{112\}\langle 241\rangle$ is also high in Fig.3.

The r -values calculated for each texture component using a software developed by Inoue are summarized in Fig.4. The predicted r -values for the $\{332\}$, $\{221\}$ and $\{112\}$ orientations are considerably high, even though they are not as high as that of the ideal $\{111\}$ orientation. Therefore, it is provable that the $\{332\}$, $\{221\}$ and $\{112\}$ orientations also have considerable effects on the improvement of the average r -value.

Another important feature for the AWRed sheets is a limited area fraction of the $\{001\}$ grains. The $\{001\}\langle 100\rangle$ orientation is rarely seen, though small amount of $\{001\}\langle 110\rangle$ exists. Since the $\{001\}$ orientations tend to decrease average r -value, it is effective to limit the amount of $\{001\}$ grains for improving average r -values. The predicted r -value for the $\{115\}\langle 110\rangle$ orientation which exists in the AWRed is rather low, but it is higher than that for the $\{001\}\langle 110\rangle$ orientation.

As a result of the modified recrystallization texture, the AA6022 alloy T4 sheet prepared by AWR actually has a high average r -value of 1.2; the r -values for RD0°, 45° and 90° are 1.0, 1.4 and 1.1, respectively. This average r -value is considerably higher than that of the CRed sheet.

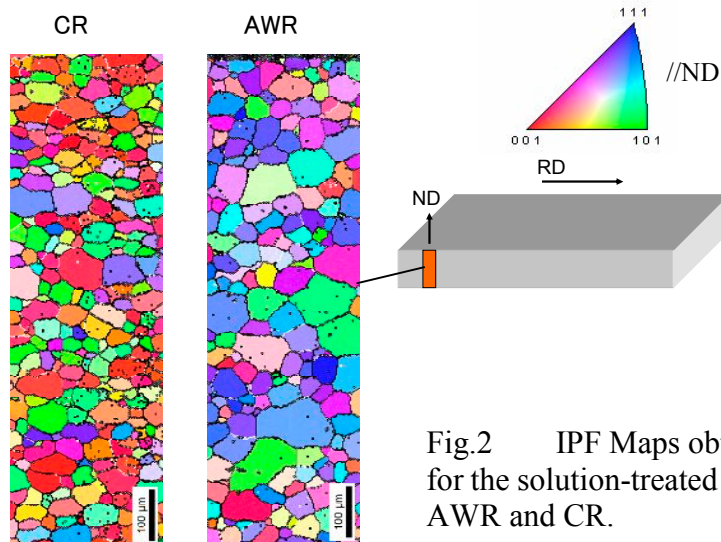


Fig.2 IPF Maps obtained by SEM-EBSD for the solution-treated T4 sheets prepared by AWR and CR.

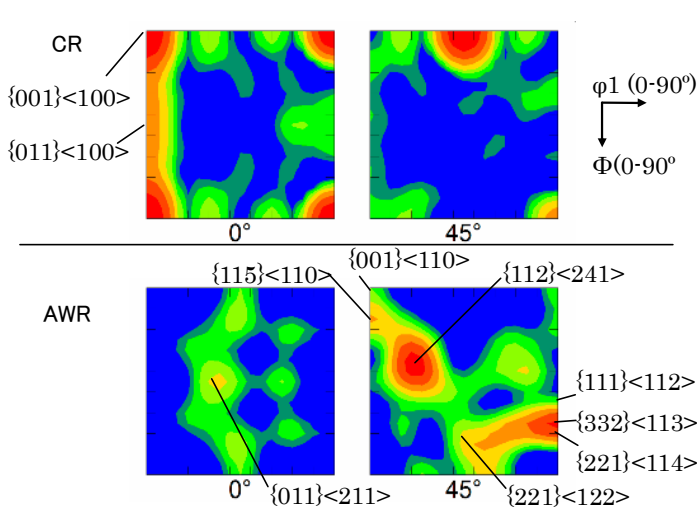


Fig.3 Recrystallization texture of the T4 sheets by AWR and CR. (ODF : $\phi_2=0^\circ$, 45° sections)

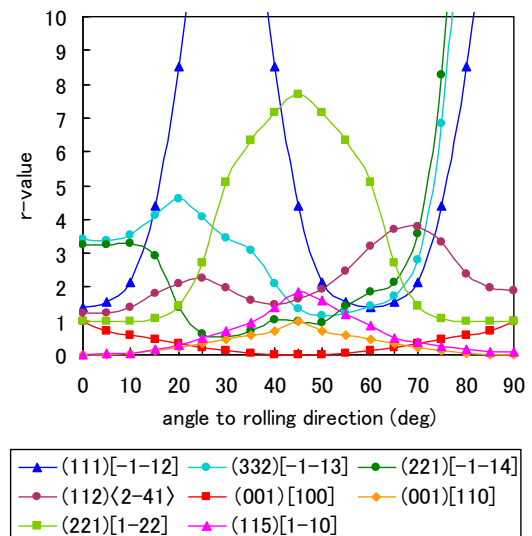


Fig.4 The r -values for various orientations predicted by using a software developed by Inoue.

3.2 Texture change during multi-step annealing

EBSD-IPF maps for the sheets by AWR are shown in Fig.5; these maps indicate the changes in the grain structure and texture in an identical area on the sheet surface during the multi-step annealing at 573–723 K. ODFs at $\phi 2=45^\circ$ calculated on the basis of the EBSD data are illustrated in Fig.6. The microstructure of the as-AWR sheet consists of subgrains or considerably recovered grains, some of which act as nuclei for the recrystallization during annealing. The texture of this sheet consists of the $\{001\}\langle 110 \rangle$ orientation and the texture fibers of $\langle 110 \rangle//RD$ and near $\langle 111 \rangle//ND$.

A completely recrystallized structure is attained after the final step of annealing at 723 K, and its texture is similar to that of the T4 sheets after SHT, although the heating conditions are different. This implies that texture evolution behavior during the multi-step annealing process is basically the same as the behavior during SHT.

The first step of annealing at 573 K leads to local recrystallization or grain growth, and the subsequent annealing steps at the higher temperatures result in the grain growth consuming the adjacent unrecrystallized area. The changes in texture are basically brought about by the preferential growth and disappearance of grains during annealing. Fig.7 shows the change in the area fraction for the $\{001\}$, $\{115\}$, $\{111\}$, $\{112\}$, $\{332\}$, and $\{221\}$ grains during the multi-step annealing process. The area fractions for the $\{115\}$, $\{112\}$, $\{332\}$ and $\{221\}$ grains are maintained or increased through the progress of recrystallization during annealing, whereas that for the $\{001\}$ grains is reduced.

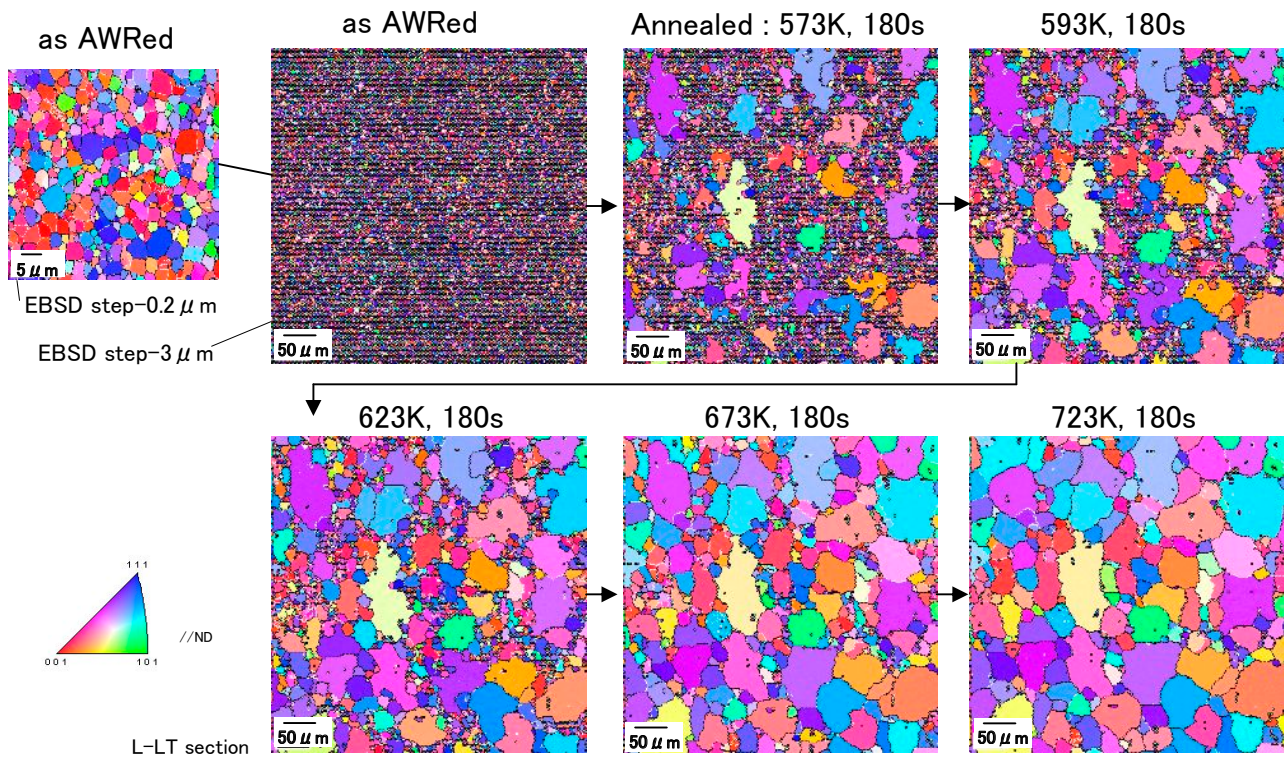


Fig.5 Microstructure change of the AWRed AA6022 sheet during multi-step annealing at 573K-723K. IPF maps obtained by SEM-EBSD for an identical observation area.

The decrease in area fraction of the $\{001\}$ grains in the AWRed sheets during recrystallization is accompanied with the growth of adjacent grains of some other orientations, e.g. $\{112\}$ and $\{221\}$. The changes in the area fraction suggest that the $\{221\}$ grains possibly grow by effectively consuming the adjacent $\{001\}$ orientation. The boundaries between the $\{221\}$ and the $\{001\}$ grains may have a high migration rate for the grain growth because $\{221\}\langle 114 \rangle$ and $\{221\}\langle 122 \rangle$ have a relationship of 60° rotation around the $\langle 111 \rangle$ axis with $\{001\}\langle 110 \rangle$ and $\{001\}\langle 100 \rangle$, respectively.

The existence of the remained $\{115\}\langle 110\rangle$ grains seems to be unfavorable for improving the r-value in a general sense. However, if the $\{115\}$ grains grow by consuming the adjacent $\{001\}$ grains, they have a slight effect on improvement of the r-value.

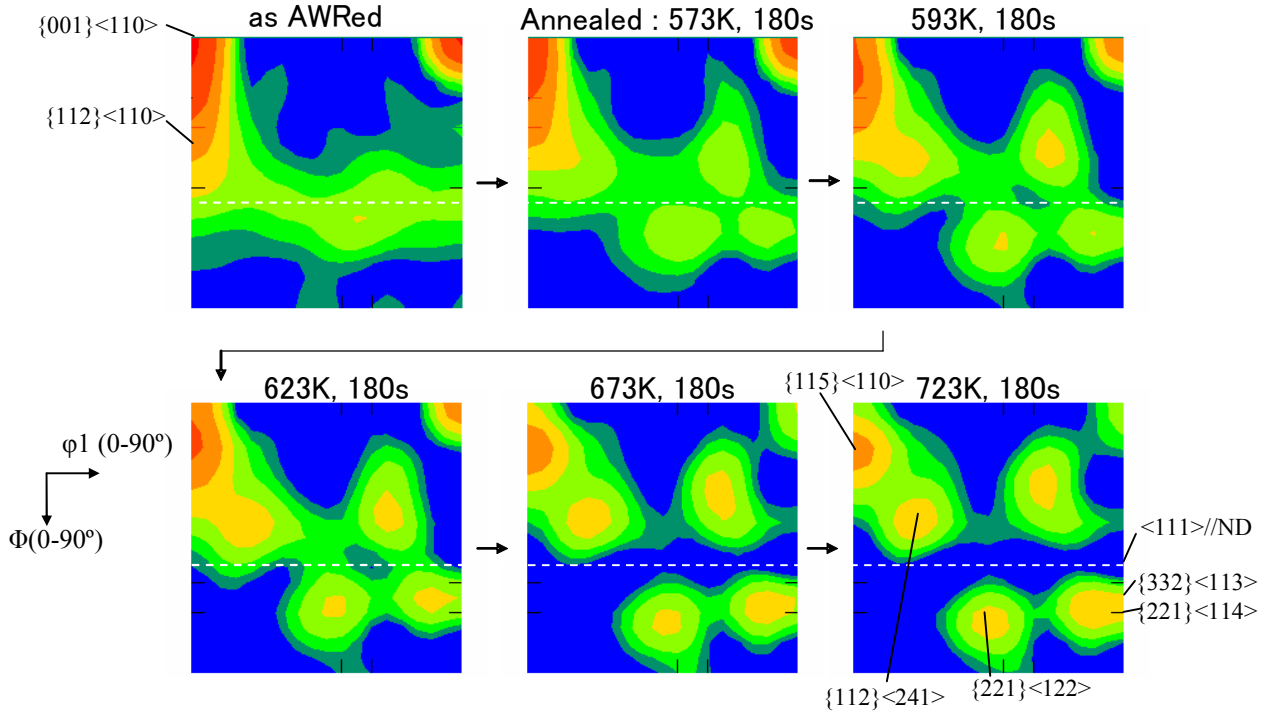


Fig.6 Changes in the texture of the AWRed AA6022 sheet during multi-step annealing at 573K-723K. (ODF from SEM-EBSD data : $\phi_2=45^\circ$ section.)

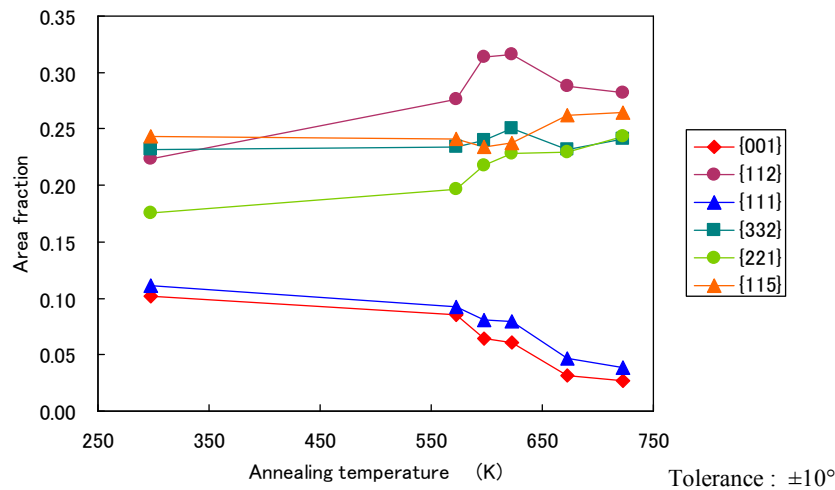


Fig.7 Changes in area fraction of the grains having the $\{001\}$, $\{115\}$, $\{112\}$, $\{111\}$, $\{332\}$ and $\{221\}$ orientations during multi-step annealing.

The $\{111\}$ orientation that is considered to be the texture component having a strong effect on the improvement of the average r-value is also decreased in area fraction during the annealing process. It is clear that the $\{111\}$ orientation is not a preferred orientation for grain growth, at least in the case of

the AA6022 sheets by AWR. Since the fraction of the ideal $\{111\}$ orientation is rather small, the high r-value of the AWRed sheets cannot be explained only by the existence of the $\{111\}$ orientation.

Consequently, the improved r-values of the sheets by AWR are caused by a combination of recrystallization texture components ; a large fraction of the orientations including $\{111\}$, $\{112\}$, $\{332\}$ and $\{221\}$ which increase r-values, and a limited fraction of $\{001\}$ orientations which lower r-values.

4. Conclusion

The AA6022 alloy sheets have a subgrain structure or a recovered structure consists of grains with the $\{001\}<110>$ orientation and the texture fibers of $<011>//RD$ and near $<111>//RD$ before the recrystallization treatment. Some of the recovered grains act as nuclei for the recrystallization, and grow by consuming the adjacent grains. The area fractions of the $\{001\}$ and $\{111\}$ grains are decreased, while those of the $\{112\}$, $\{332\}$ and $\{221\}$ grains are maintained or increased through recrystallization during the multi-step annealing process. The $\{221\}$ grains possibly grow in a preferential manner consuming $\{001\}$ grains during recrystallization. Not only the ideal $\{111\}$ orientation but also the $\{112\}$, $\{332\}$ and $\{221\}$ orientations probably have an effect on the improvement of the r-value of the recrystallized sheets. The limited fraction of the $\{001\}$ grains is another reason for the high r-value of the AWRed sheets.

5. Acknowledgements

The authors acknowledge NEDO (New Energy and Industrial Technology Development Organization) for its support to this work under the research project titled “Aluminum Production and Fabrication Technology Development Useful for Automotive Light-Weighting”. We wish to express our gratitude to Ass. Prof. Hirofumi Inoue at Osaka Prefecture University for helpful suggestions.

References

- [1] O. Noguchi, T. Komatsubara *et al.*: Proc. 9th Int. Conf. on Al Alloys, (2004) 758-762.
- [2] Y. Suzuki, T. Omura, S. Hirosawa, T. Sato: Mater. Sci. Forum Vol.519-521 (2006) 1505-1510.
- [3] Y. Miki, K. Koyama *et al.*: Mater. Sci. Forum Vol.539-543 (2007) 333-338.